Lithium-induced dimer reconstructions on Si(001) studied by photoelectron spectroscopy and band-structure calculations

P. E. J. Eriksson,[1] Kazuyuki Sakamoto,[2] and R. I. G. Uhrberg[1]
[1]*Department of Physics, Chemistry and Biology, Linköping University, S-581 83 Linköping, Sweden*
[2]*Graduate School of Science and Technology, Chiba University, Chiba 263-8522, Japan*
(Received 23 October 2006; revised manuscript received 2 March 2007; published 10 May 2007)

The electronic and atomic structure of Si(001) with 0.5 and 1 ML of lithium have been studied experimentally using angle resolved ultraviolet photoelectron spectroscopy, Si 2*p* core level spectroscopy, and low energy electron diffraction. Experimental surface state dispersions are compared with recent theoretical results in the literature and with results from additional density functional theory calculations. Four adsorption configurations for the 0.5 ML 2×2 surface and three configurations for the 1 ML 2×1 surface are compared. Fittings of Si 2*p* core level data support the alternation of strongly and weakly buckled Si dimers of the 2×2 models and symmetric Si dimers of the 2×1 models based on the relative intensities of the surface components. As a tool to differentiate between the different 2×2 and 2×1 models surface state dispersions are used since they are sensitive to the positions of the Li adatoms.

DOI: 10.1103/PhysRevB.75.205416 PACS number(s): 73.20.At, 79.60.−i, 68.43.−h

I. INTRODUCTION

Alkali metal (AM) adsorption on Si(001) surfaces has attracted much attention for decades due to its potential as a prototype system for metal-semiconductor interfaces. There has been much discussion on the character of the Si-AM bond, the buckling of the Si dimers, the saturation coverage, and the adsorption sites over the years. Levine's[1] early work proposed AM adsorption in linear chains with adatoms at the pedestal (*P*) sites and a saturation coverage of 0.5 monolayer (ML). Later, this was challenged by Enta *et al.*[2] who found the saturation coverage of K on Si to be 1 ML and proposed a double layer model for the adsorption. This was confirmed by Abukawa and Kono[3] based on x-ray diffraction measurements on the Si(001):K surface. In the double layer model AM adatoms sit both at the *P* site and in the trough between the Si dimer rows. This gives a saturation coverage of 1 ML compared to 0.5 ML in Levine's model. The position of the AM in the trough and the degree of buckling of the dimers in the double layer model are two issues that are still under discussion.

Li adsorption at around 0.5 ML coverage on Si(001) induces a 2×2 phase[4] which is not observed with the other AM. Calculations by Shi *et al.*[5] and Ko *et al.*[6] suggest different configurations for the Li atoms in the 2×2 surface unit cell. Shi *et al.*[5] suggested two configurations based on total energy calculations. The first model is depicted in Fig. 1(a) along with the high symmetry sites *P*, *B*, and *T*4. In this model one Li adatom occupies a *B* site, and the second Li adatom sits close to a *T*4 site. Shi *et al.*[5] also suggested a configuration with the first Li adatom at a site close to *P* but shifted towards the *B* site. Such a site is denoted *P'*. The position of the second Li adatom is the same as in the first model. Ko *et al.*[6] proposed a model with Li adatoms in linear chains occupying both of the sites in the 2×2 unit cell that are similar to *B*. Both models correspond to a 0.5 ML coverage of Li. All these models of the 2×2 surface contain one strongly buckled and one weakly buckled Si dimer per unit cell.

For the 1 ML Li 2×1 surface most models agree on *P* as one adsorption site. Several suggestions have, however, been made for an adsorption site in the trough. Morikawa *et al.*[7] reported the *T*3 site as the most stable one, Ko *et al.*[6] found the *T*4 site favorable while Kobayashi *et al.*[8] and Shi *et al.*[9] suggested two similar sites close to the midpoint between the *T*3 and *T*4 sites as the configurations with the lowest energy. The model by Shi *et al.*[9] is shown in Fig. 1(b) along with the high symmetry sites *P*, *T*3, and *T*4. The Si dimers were reported to be buckled judging from the Si 2*p* core level shifts (CLS) identified by Kim *et al.*[4] while Si 2*p* CLS data of Grehk *et al.*[10] as well as most theoretical studies support models with symmetric Si dimers.

In this paper we present surface band dispersions obtained by angle resolved photoelectron spectroscopy (ARPES) and compare to recent band-structure calculations by Shi *et al.*[5,9] for the 2×2 and 2×1 Si(001):Li surfaces. We also present results from additional band-structure calculations in the [010] direction. Surface state dispersions of 2×2 models that are very close to those suggested by Shi *et al.*,[5] denoted *B*-*T*4 and *P'*-*T*4, and Ko *et al.*,[6] denoted *P'*-*P'* and *B*-*B*, are compared to experimental results in the [010] direction. The same kind of comparison is presented for three 2×1 models which are very similar to those suggested by Shi *et al.*,[9] Morikawa *et al.*,[7] and Ko *et al.*[6] The three 2×1 models are denoted *P*-*T*3', *P*-*T*3, and *P*-*T*4, respectively. *T*3' denotes a site close to the midpoint between *T*3 and *T*4. In addition, high resolution Si 2*p* core level data are presented that support the models with alternating strongly and weakly buckled dimers for the 0.5 ML 2×2 surface and symmetric dimers for the 1 ML 2×1 surface.

II. EXPERIMENTAL DETAILS

The experimental part of this work was conducted at the MAX-lab synchrotron radiation facility in Lund, Sweden. ARPES measurements were done at beamline 33 at the MAX-I storage ring. Linearly polarized photons with $h\nu$ =21.2 eV were used throughout the angle resolved measure-

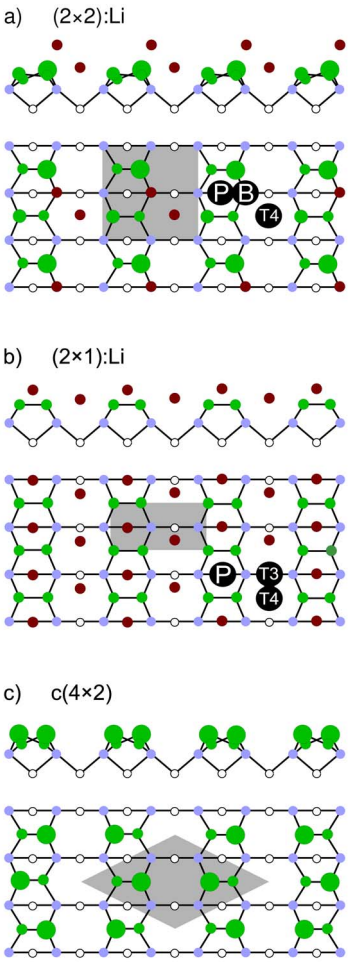

FIG. 1. (Color online) Atomic structure of (a) *B*-*T*4 (2×2):Li by Shi *et al.* (Ref. 5), (b) *P*-*T*3′ (2×1):Li by Shi *et al.* (Ref. 9) and (c) clean $c(4\times2)$. Large dimer atoms indicate up atoms, while small indicate down atoms. The difference in size between the atoms forming a dimer indicates the degree of buckling. The surface unit cell is drawn for each model. Four sites are marked, *P*: pedestal, *B*: above second layer Si, *T*3: above third layer Si, and *T*4: above fourth layer Si.

ments. The experimental energy resolution was about 80 meV and the angular resolution was ±2°. The Si 2*p* core level spectra presented here were obtained at beamline I311 at the MAX-II storage ring. The experimental energy resolution using a photon energy of 145 eV was about 30 meV. The Si(001) samples (*n*-doped, P) used in the experiments were cut from two single crystal wafers into (1) off-axis sample $\rho=1-10\ \Omega$ cm, cut with the macroscopic surface normal 4° off the [001] direction used for ARPES in the [110] and $[\bar{1}10]$ directions and (2) on-axis sample, $\rho=1.7-2.4\ \Omega$ cm, used for core level studies and ARPES in the [010] direction. The sample temperature was kept at ≈100 K during all data taking and Li adsorption. The pressure was below 3×10^{-10} Torr during the measurements. Sample preparation was similar for both the valence band and the core-level measurements. Cleaning was done via direct resistive heating up to 1250 °C in order to remove any carbon contamination. Annealing to 930 °C for 30 s was

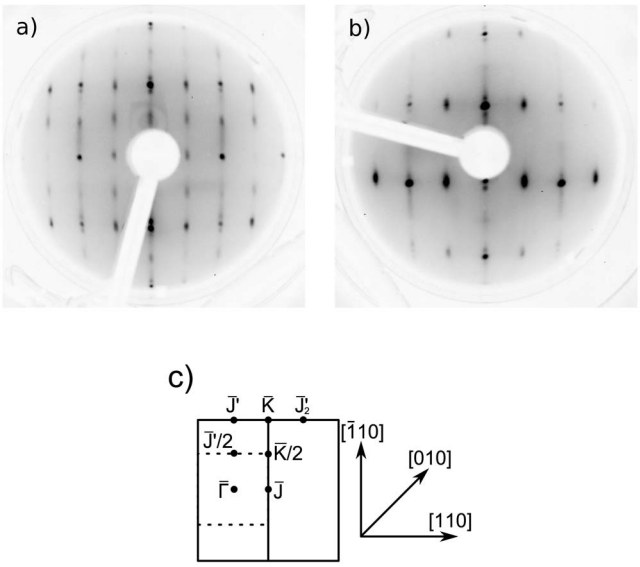

FIG. 2. LEED pattern from the 4° off-axis sample obtained at 99 eV electron energy of (a) a 0.5 ML Li 2×2 surface and (b) a 1 ML Li 2×1 surface. (c) Surface Brillouin zones of the 2×1 and 2×2 surfaces drawn by solid and dotted lines, respectively.

routinely done to remove Li between exposures. Li was evaporated from a commercial getter source (SAES getters) positioned 4 cm from the sample. The evaporation time was accurately controlled by a shutter in front of the source. The Li coverage was estimated from the work function change and the low-energy electron diffraction (LEED) pattern. The change in work function was found to be consistent with previous results[11] for the different surface reconstructions and Li coverages. The Fermi energy of a Ta foil in electrical contact with the sample was used as reference in the ARPES measurements. All low temperature data were obtained while flooding the sample with white light from an external source in order to remove any band bending. To compensate for the surface photovoltage shift all valence band spectra have been shifted by 0.4 eV to facilitate direct comparisons with room temperature data.

Figure 2(a) shows the LEED pattern obtained from the 2×2 surface prepared on the 4° off-axis Si(001) sample. In Fig. 2 the orientation of the LEED patterns is such that the $\bar{\Gamma}$-$\bar{J}$ direction is horizontal. The splitting of the spots in the $[\bar{1}10]$ direction is due to a regular array of steps on the surface. Intensity analysis of the 2×1 LEED pattern from the clean surface at room temperature indicates that the majority domain constitutes 80% of the surface. The 2×2 pattern shown in Fig. 2(a) might also contain contributions from patches with the higher Li coverage 2×1 reconstruction. Several surfaces were prepared that showed 2×2 LEED patterns and the measured dispersions on the different surfaces are consistent despite minor variations in the work function change.

Figure 2(b) shows the LEED pattern obtained from the 2×1 surface. Apart from the split spots in the $[\bar{1}10]$ direction due to the regular step structure on the surface there is also a slight streakiness in the same direction. This is suspected to be related to irregularities of the step structure. No

traces of the lower Li coverage 2×2 nor of the higher Li coverage $c(3\sqrt{2}\times\sqrt{2})$R45° phases[11] can be seen in Fig. 2(b).

III. COMPUTATIONAL DETAILS

Several Li/Si(001):2×2 and Li/Si(001):2×1 models proposed earlier in the literature are used for comparisons with our experimental results. Figures 1(a) and 1(b) show the 2×2 and 2×1 structures, respectively. Figure 1(c) shows the clean Si(001) $c(4\times2)$ reconstruction for comparison. The magnitude of the tilt of the dimers is illustrated by the different sizes of the dimer atoms. A larger difference in size indicates a larger tilt angle. The 2×2 models consist of dimers with an alternating tilt direction along the dimer rows as well as a difference in the magnitude of the tilt angle. Weakly buckled dimers alternate with strongly buckled dimers as shown in Fig. 1(a) where the Li adsorption sites of the *B*-*T*4 model have also been marked. The 2×1 models are made up of symmetric Si dimers, which, along with the Li adsorption sites of the *P*-*T*3′ model is shown in Fig. 1(b).

In the [010] direction, we have calculated surface state dispersions of four 2×2 models, *P*′-*T*4, *B*-*T*4, *P*′-*P*′, and *B*-*B*, and three 2×1 models *P*-*T*3′, *P*-*T*3, and *P*-*T*4. The calculated band structures in the [010] direction presented in Sec. IV A 3 in this paper were obtained by density functional theory calculations in the generalized gradient approximation[12] using the full-potential (linearized) augmented plane-wave+local orbitals method within the WIEN2k code.[13]

The 2×2 and 2×1 structures were modeled with 13 Si layers. The slabs were mirrored in the [001] direction with Si dimer reconstruction and Li adatoms on both sides. A vacuum of about 12 Å was used to separate the slabs in the [001] direction. The structure was periodically repeated in all directions. The self consistent field procedure was performed using eight k points in the irreducible Brillouin zone. The plane wave expansion cutoff was about 75 eV and the calculated band structure showed very little variation when changing the cutoff. Additional total energy comparisons of the 2×2 structures were performed with 109 and 129 eV energy cutoffs. Different cutoffs did not change the sign of the total energy differences. Using the atomic configurations proposed in Refs. 5–7 and 9 as input data the structures were allowed to relax using the WIEN2k code in order to obtain as reliable results as possible. The relaxation resulted in only very minor changes of the positions of the atoms, as these configurations were found to be very close to stable local energy minima.

IV. RESULTS AND DISCUSSION

A. Surface band structure

1. Li/Si(001):2×2 along [$\bar{1}$10] and [110]

The photoemission data, shown in Fig. 3, of the surface states in both the $\bar{\Gamma}$-$\bar{J}'$ and $\bar{\Gamma}$-$\bar{J}$ directions on the 2×2 surface show great similarities with ARPES data from the clean $c(4\times2)$ surface. At the $\bar{\Gamma}$ point only one component has been marked S_1, 1 eV below E_F. The large width of the peak

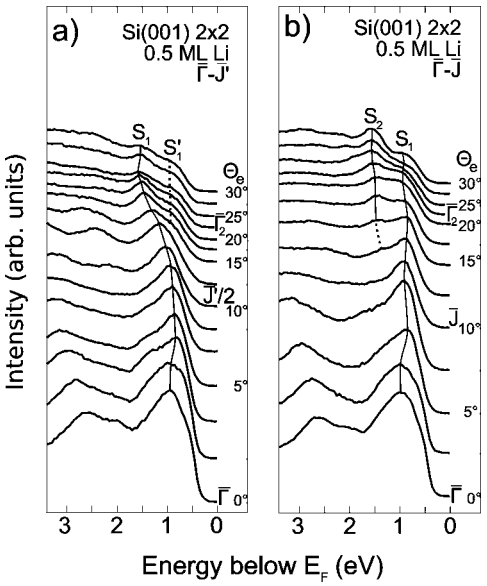

FIG. 3. Photoemission spectra recorded on the 2×2 Li-induced surface for different emission angles using $h\nu$=21.2 eV. (a) Spectra taken along $\bar{\Gamma}$-$\bar{J}'$/2-$\bar{\Gamma}_2$. (b) Spectra taken along $\bar{\Gamma}$-$\bar{J}$-$\bar{\Gamma}_2$. Solid (dotted) lines indicate clear (weak) features.

does however suggest that it may consist of several components.

Figure 3(a) shows spectra obtained along the dimer rows ($\bar{\Gamma}$-$\bar{J}'$ direction). A strong feature S_1 starts out at about 1 eV below E_F at $\bar{\Gamma}$ and can be followed dispersing downwards to reach about 1.55 eV at the $\bar{\Gamma}$ point of the second surface Brillouin zone (SBZ). Near $\bar{J}'/2$ a weak shoulder marked S_1' becomes visible and it can be followed at larger values of $k_\parallel$ but no dispersion can be resolved. In the $\bar{\Gamma}$-$\bar{J}$ direction two bands with small dispersions are marked in Fig. 3(b). For small $k_\parallel$ values only the S_1 state at about 1 eV below E_F can be seen but for larger $k_\parallel$ values, beyond the $\bar{J}$ point, it is possible to resolve an additional component S_2 at 1.5–1.6 eV below E_F.

When going from the clean $c(4\times2)$ to the 0.5 ML Li-induced 2×2 surface the largest difference in the surface band structure is a rigid shift towards increased binding energy by about 0.3 eV. This is similar to the observation by Kim *et al.*[4] The general band dispersions are very similar to ARPES data from the clean surface. This indicates that only a small rearrangement of the dimer structure has occurred.

Figure 4 shows a comparison between our experimental data and the theoretical results of Shi *et al.*[5] Calculated surface states derived from dangling bonds on the Si dimer atoms are denoted by asterisks, empty diamonds, and empty squares. It is difficult to see any symmetry in the dispersions around the first SBZ boundaries, represented by the $\bar{J}$ and $\bar{J}'/2$ points in Figs. 3 and 4 where the experimental data show more of a 2×1 symmetry. One possibility is that the symmetry is obscured by overlap with the bulk bands. In the $\bar{\Gamma}$-$\bar{J}$ direction all surface related bands overlap with the projected bulk bands. The same is true for $\bar{\Gamma}$-$\bar{J}'$, except for a

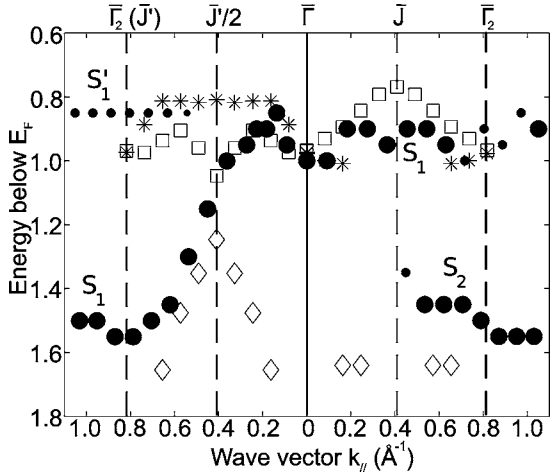

FIG. 4. Theoretical and experimental surface state dispersions on the 2×2:Li surface. Large (small) solid circles indicate strong/clear (weak) experimental features while asterisks, empty diamonds and empty squares are theoretical results by Shi *et al.* (*B-T*4 model) (Ref. 5). Symmetry points have been marked with dashed lines.

small region near $\bar{J}'$ where the surface bands are separated from the bulk bands. A combination of the calculated bands marked with squares between $\bar{\Gamma}$ and $\bar{J}'/2$ and diamonds between $\bar{J}'/2$ and $\bar{\Gamma}_2$ fit quite well with the experimental dispersion of the S_1 band in the $\bar{\Gamma}$-$\bar{J}'/2$-$\bar{\Gamma}_2$ direction. In the $\bar{\Gamma}$-$\bar{J}$ direction the behavior of S_1 is qualitatively reproduced by the calculated bands shown by open squares. The lower band S_2 cannot be found in the calculated surface band structure.

2. Li/Si(001):2×1 along [$\bar{1}$10] and [110]

Figure 5(a) shows the results from the $\bar{\Gamma}$-$\bar{J}'$ direction, i.e., along the dimer rows. Two features are indicated in the spectra. A strong feature, S_2 1.5 eV below E_F at the $\bar{\Gamma}$ point seems to initially show an upward dispersion to $k_{\|}=0.3$ Å^{-1} ($\theta_e\approx8°$). It then turns downwards toward a minimum of 1.7 eV below E_F at the $\bar{J}'$ point. A weaker feature S_1', seen as a shoulder with a binding energy of 1 eV, is marked in Fig. 5(a) by a dotted line. It shows very little dispersion and is attributed to contributions from the minority domain. It corresponds to the flat S_1 band 1 eV below E_F in the $\bar{\Gamma}$-$\bar{J}$ direction, see Fig. 5(b). The region around $\theta_e\approx7.5°$ is better resolved compared to earlier work[4] as we are able to follow the S_1' shoulder in all the spectra. This results in a higher binding energy of S_2 at low emission angles than what was reported in Ref. 4. Along $\bar{\Gamma}$-$\bar{J}$ two features S_1 and S_2' about 1 and 1.5 eV below E_F show very little dispersion as shown in Fig. 5(b). The S_1 component making up the shoulder at the $\bar{\Gamma}$ point is well defined close to the $\bar{\Gamma}$ point of the second SBZ. S_2' is difficult to follow and is attributed to the minority domain. Near $\bar{\Gamma}$ the S_2 state is visible. At an emission angle of 7.5° it is not possible to resolve the two components as the spectrum just shows a broad peak.

In Fig. 6 the dispersions along the $\bar{\Gamma}$-$\bar{J}'$ and $\bar{\Gamma}$-$\bar{J}$ directions derived from Fig. 5 are compared to the theoretical results of

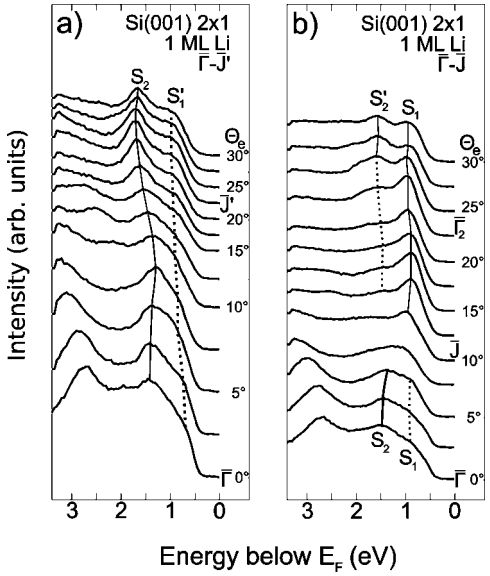

FIG. 5. Photoemission spectra recorded on the 2×1 Li-induced surface for different emission angles using $h\nu=21.2$ eV. (a) Spectra taken along $\bar{\Gamma}$-$\bar{J}'$. (b) Spectra taken along $\bar{\Gamma}$-$\bar{J}$-$\bar{\Gamma}_2$. Solid (dotted) lines indicate clear (weak) features.

Shi *et al.*[9] Asterisks, empty triangles, and empty squares are the calculated dispersions of surface states derived from dangling bonds on the Si dimer atoms. The theoretical data have been shifted down by 0.3 eV to match the experimental data. The lower band S_2, showing symmetry around $\bar{J}'$, is consistent with the theoretical results (empty squares). In the experiment it is only possible to find one of the dispersing bands along $\bar{\Gamma}$-$\bar{J}'$, described in the calculation. The upper experimental band S_1' near the $\bar{J}'$ point and S_1 near $\bar{\Gamma}_2$ show similar behavior. This supports the assignment of S_1' to contributions from the minority domain. The feature found

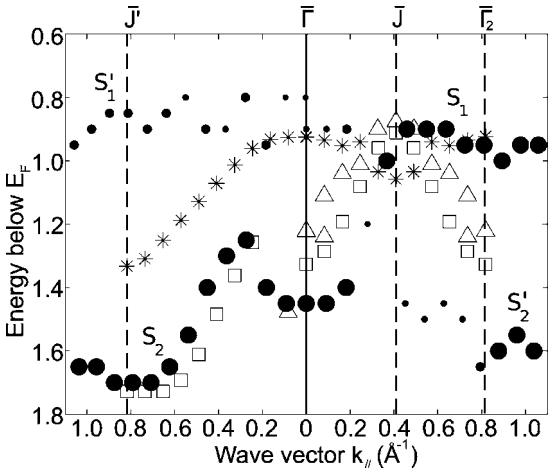

FIG. 6. Theoretical and experimental surface state dispersions on the 2×1:Li surface. Large (small) solid circles indicate strong/clear (weak) experimental features while asterisks, empty triangles, and empty squares are theoretical results by Shi *et al.* (*P-T*3′ model) (Ref. 9). Symmetry points have been marked with dashed lines.

1.45 eV below E_F at the $\bar{\Gamma}$ point is also expected at $\bar{\Gamma}_2$. A band S_2' is, however, found at about 0.1 eV higher binding energy. This behavior could be explained by overlap with the S_2 band at 1.7 eV from the minority domain which would cause a shift in the peak position. The S_2' feature in the spectra from the region near $\bar{\Gamma}_2$, Fig. 5(b), is quite broad which supports such an explanation. The behavior of the band about 1.5 eV below E_F near $\bar{\Gamma}$ is not very well reproduced in the theoretical data. The bulk band structure completely overlaps the surface related features on this surface in the $\bar{\Gamma}$-$\bar{J}$ direction and in the $\bar{\Gamma}$-$\bar{J}'$ direction. The surface related structure is separated from the bulk bands only in a small region about 0.1 Å^{-1} around $\bar{J}'$.

3. Li/Si(001):2×2 and Li/Si(001):2×1 along [010]

To further test the 2×2 and 2×1 models we have performed ARPES measurements using an on-axis Si(001) sample. A sample with the macroscopic surface normal along a principal axis will have less defects than a sample where the normal is 4° off because of the surface step structure on the off-axis sample. The disadvantage to use an on-axis sample is that the ratio between the two domains is close to 1. In these measurements we have probed the SBZ in the [010] azimuth, see Fig. 2(c), which contains equivalent $k_\parallel$ points in both domains. According to calculations the surface bands are more separated from the bulk bands in this direction in the SBZ. This increases the possibility to identify the surface states. LEED patterns obtained from the on-axis sample showed very nice 2×2 and 2×1 spots for the 0.5 ML Li and 1 ML Li-induced surfaces, respectively. The quality of the surfaces prepared on the on-axis sample was notably better compared to those prepared on the off-axis sample judging from the LEED patterns.

Figure 7 shows ARPES spectra along the [010] azimuth obtained from the 2×2 and 2×1 Li surfaces prepared on the on-axis sample. The 2×2 surface shows dispersions very similar to the clean surface. As in the case of the off-axis sample there is a downward shift of the surface states by about 0.3 eV compared to the clean Si(001) surface. A strong feature, marked S_1 in Fig. 7(a), shows symmetry both around a point halfway between $\bar{\Gamma}$ and $\bar{K}/2$ and around $\bar{\Gamma}_2$. At higher emission angles, beyond the $\bar{K}/2$ point, one can resolve a weak band S_1' at lower binding energy which shows symmetry around $\bar{\Gamma}_2$. On the 2×1 surface, shown in Fig. 7(b), a weak S_1 and a stronger S_2 structure at ≈0.8 eV and ≈1.4 eV below E_F can be seen at the $\bar{\Gamma}$ point. They are, however, difficult to follow as they merge into a broad feature. From $k_\parallel \approx 0.4$ Å^{-1} ($\Theta_e \approx 10°$) it is again possible to follow a strong feature S_3 which starts with a slight upward dispersion and reaches a maximum of 1 eV near the SBZ boundary at $k_\parallel \approx 0.58$ Å^{-1} ($\Theta_e \approx 16°$) and then disperses downwards. At higher emission angles, around $\bar{J}_2'$, two components can be resolved at 1.4 and 1.65 eV below E_F. Both components show clear symmetry around the $\bar{J}_2'$ point. In the data from the off-axis sample only the S_2 band was found, see Fig. 6.

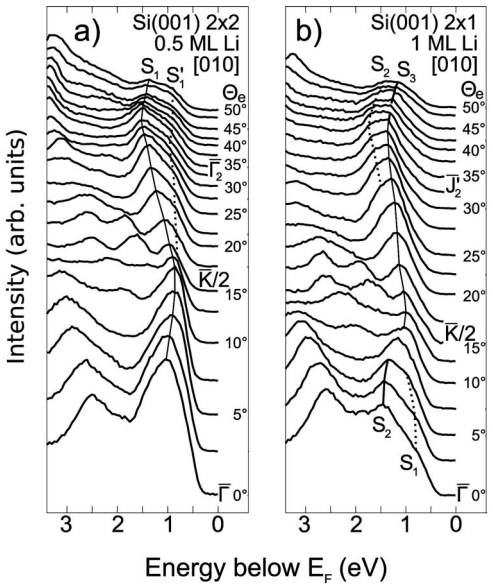

FIG. 7. Spectra obtained from a two domain on-axis sample when probed along the [010] azimuth. (a) Spectra from the 2×2:Li surface. (b) Spectra from the 2×1:Li surface.

Results from our calculations of the dispersions in the [010] azimuth on the 2×2 surface are compared to experimental band structures in Fig. 8(a). We find best agreement with experimental data and the results by Shi *et al.*[5] when using the *B*-*T*4 and *P*′-*T*4 models. Shi *et al.*[5] reported virtually identical band structures for their *B*-*T*4 and *P*′-*T*4 models while, in our calculations, they are similar but do not overlap exactly. In Fig. 8(a) dark-, medium-, and light-gray solid (dashed) lines represent three calculated surface bands of different origin obtained using the *B*-*T*4 (*P*′-*T*4) models. All three bands are of dangling bond character mainly made up of π-like orbitals on the Si dimer atoms. The dark gray band comes from orbitals mainly at the up atoms of the strongly buckled dimers but also to a smaller extent from the down atoms of the weakly buckled dimers. The medium gray band comes from the up atoms of the strongly buckled dimers and from the down atoms of the weakly buckled dimers. The light gray band comes mainly from the up atoms of the weakly buckled dimers and to a smaller extent from the down atoms of those dimers. The experimental data follow the dark gray band quite nicely but also the medium gray band of both models at $k_\parallel$ beyond the SBZ boundary at $\bar{K}/2$. The light gray band of *B*-*T*4 between $\bar{\Gamma}$ and $\bar{K}/2$ fits the experimental dispersion better than that of *P*′-*T*4. Near $\bar{\Gamma}_2$ it was not possible to identify the medium gray band of *B*-*T*4. Here the surface band of *P*′-*T*4 fits better with the relatively strong experimental feature at 1.5 eV. Some remarks concerning the effect of the Li adsorption sites can be made by comparing the calculated band structures of the *P*′-*T*4, *B*-*T*4, *P*′-*P*′, and *B*-*B* models, shown in Fig. 8(b). It can be noted that our dispersions using the *B*-*B* model are very similar to the results by Ko *et al.*[6] using the same model. The bands found between 0.65 and 0.75 eV below E_F near $\bar{K}/2$ using the *P*′-*P*′ and the *B*-*B* models are not observed in the experiments. An increased split of the bands can be observed

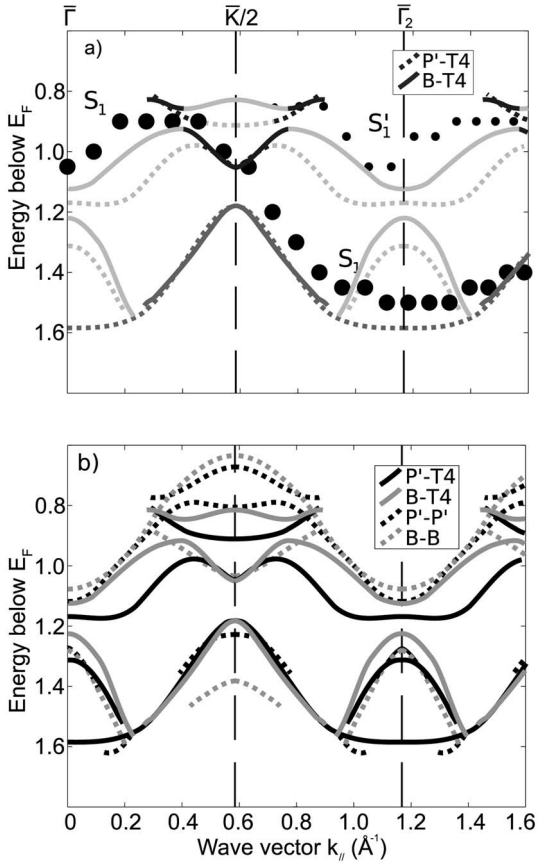

FIG. 8. Comparison between calculated band structures (lines) and experimental dispersions (solid circles) in the [010] azimuth on a two domain on-axis 0.5 ML Li 2×2 Si(001) surface. Large (small) solid circles indicate strong/clear (weak) features in the experiment. (a) Dark, medium, and light gray bands indicate bands of different origin using the P'-$T4$ and B-$T4$ models drawn with dotted and solid lines, respectively. (b) Comparison of calculated surface band structures of the P'-$T4$, B-$T4$, P'-P', and B-B models drawn with solid dark, solid light, dotted dark, and dotted light lines, respectively.

near the SBZ boundary at $\bar{K}/2$ when changing from $T4$ to P' and B models [solid to dotted curves in Fig. 8(b)]. Total energy comparisons showed a difference on the order of 10 meV per 2×2 cell between B-$T4$ and P'-$T4$, favoring B-$T4$. This, in combination with the very similar band structures, makes these models indistinguishable. The B-B and P'-P' models give on the order of 100 meV higher total energies. Calculations performed with additional accuracy only changed the differences by a few meV.

On the 2×1 surface two calculated bands obtained using the P-$T3'$ model are drawn with dark gray lines in Fig. 9. Near $\bar{\Gamma}$ only one band is identified due to overlap with bulk bands. It starts with an upward dispersion from $\bar{\Gamma}$ and then it turns downwards. About 0.4 Å^{-1} out an additional band at $\approx$0.15 eV higher binding energy is found. The splitting between the bands increases with $k_{\parallel}$ and is 0.3 eV at the $\bar{J}_2'$ point. This is similar to the 0.4 eV split at $\bar{J}'$ in the calculation reported in Ref. 9, shown in Fig. 6. We have characterized the contributions to both of the calculated bands and

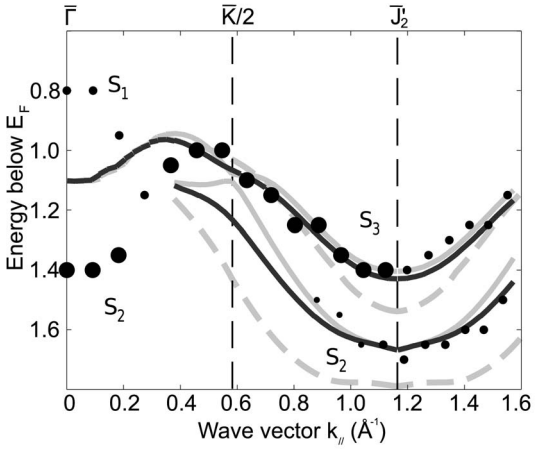

FIG. 9. Comparison between calculated band structures (lines) and experimental dispersions (solid circles) in the [010] azimuth on a two domain 1 ML Li 2×1 Si(001) surface. Large (small) solid circles indicate strong/clear (weak) features in the experiment. The dark gray, solid light gray and dashed light gray bands are obtained using the P-$T3'$, P-$T3$, and P-$T4$ models, respectively.

found them to be mostly made up of π-like orbitals on the Si dimer atoms, similar to the character of the calculated bands in Fig. 6. From $\bar{\Gamma}$ and about 0.3 Å^{-1} towards $\bar{J}_2'$ bulk bands overlap with the surface related features in the calculations and this might explain the discrepancy between experiment and calculations in this range.

Comparisons with the experimental results show generally good agreement in the [010] azimuth for the 2×1 P-$T3'$ model. There is a good match between theory and experiment regarding the S_3 band. The S_2 band which in the experiment shows up as a weak feature near $\bar{J}_2'$ is reproduced in the calculated band structure. Two experimental features are missing in the calculated dispersions. First, the downward dispersing weak S_1 feature which may be bulk related since it approximately follows the edge of the calculated bulk bands and second, the behavior of S_2 near $\bar{\Gamma}$ is not reproduced.

The calculations using the P-$T3'$ model do not give any explanation as to why S_2 is not seen near $\bar{K}/2$. The photoemission data in Fig. 7(b) reveal a sharpening of the identified surface state close to $\bar{K}/2$. This is not fully consistent with the calculated results using the atomic configuration of the P-$T3'$ model, see Fig. 1(b), for which the bands remain well separated near the SBZ boundary. We therefore calculated the surface state band structure of other 2×1 models. Using the P-$T3$ model our calculations give significantly different dispersions in the [010] direction. The surface band structure obtained using the P-$T3$ model is drawn with solid light gray lines in Fig. 9. Using this model the bands move closer together near $\bar{K}/2$. In the other models P-$T4$ and P-$T3'$, the bands are more separated. The bands obtained using the P-$T4$ model (dashed light gray lines in Fig. 9) show the largest separation.

We can summarize the results concerning the electronic structure in the [010] azimuth. Among the 2×2 models we found that it was difficult to pick out a single model. Instead we found that B-$T4$ and P'-$T4$ are the most likely. The sur-

face band structures of the 2×1 models differ in the split between the bands at the SBZ boundary. Using this as a critical test we find that the *P-T*3 model is the best candidate.

B. Si 2*p* core level

The Si 2*p* core level of an on-axis Si(001) sample has been probed using photon energies between 120 and 150 eV. Normal emission was used for all measurements and the analyzer acceptance was ±8°. The spectra have been decomposed into doublets of Voigt shaped functions. A spin-orbit split of 601 meV and a Lorentzian width of 75 meV have been applied and were kept constant in all fittings. The latter was determined by fitting the low binding energy tail of the spectrum from the clean $c(4\times2)$ surface where there is only contribution from one component. This value is within the range of what has previously been reported.[14,15] Energy positions, Gaussian widths and branching ratios were varied. A good fit was characterized by (1) consistent relative energy positions of the components for the various spectra obtained using different photon energies, (2) reasonable Gaussian widths and not too big a spread among the components, and (3) branching ratios near 0.5. The number of components was determined as the lowest number for which a good fit could be obtained. The background was modeled as either integrated for the higher photon energies or exponential for the lower excitation energies.

Figure 10(a) shows the decomposition of a Si 2*p* spectrum from the clean Si(001) surface obtained at a temperature of around 100 K. All spectra presented here were taken with a photon energy of 145 eV as the spectra show the most details at this excitation energy. Six components have been used to fit the clean spectrum. The binding energies are relative to the bulk component, denoted *B*. S_u at −0.49 eV is attributed to the up atoms of the dimers, *C* at −0.2 eV has been suggested to originate from half of the third layer atoms,[14–16] S_d at 0.073 eV is attributed to the down atoms of the dimers, S' at 0.22 eV comes from the second layer atoms, and finally, *D* at 0.3 eV whose origin has not yet been determined. Gaussian widths range from 106 meV for the bulk component to 146 meV for the S_u component. The relative integrated intensities of the different fitting components are consistent with those reported in a recent study.[14]

Figures 10(b) and 10(c) show decompositions of the spectra from the Si(001) surface with the 0.5 ML Li-induced 2×2 reconstruction and the 2×1 reconstruction with 1 ML of Li, respectively. There is a notable broadening and less features compared to the spectrum from the clean $c(4\times2)$ surface. For the Li exposed surfaces good fits were achieved with four surface components and the bulk component *B*. For the 2×2 surface in Fig. 10(b) the components are S_{u+s} at −0.466 eV, C' at −0.223 eV, S'' at 0.199 eV, and D' at 0.376 eV. Gaussian widths now range from 185 meV for the bulk component to 278 meV for the component labeled S_{u+s}. On the 2×1 surface in Fig. 10(c) the relative binding energies of the components are S_s at −0.395 eV, C' at −0.215 eV, S'' at 0.219 eV, and D' at 0.374 eV. At this coverage the Gaussian widths range from 164 meV for the bulk component to 220 meV for the S_s and S'' components. Judging from the Gaussian widths, the 2×1 surfaces that were prepared in this study were of better quality than the 2×2 surfaces. The 2×2 surfaces also showed a higher degree of degradation with time. At 0.5 ML coverage the surface is more reactive than at saturation coverage so higher sensitivity to contamination is expected. The largest relative intensity of the bulk component *B* is found for the 2×2 surface with 0.5 ML Li coverage followed by the 2×1 1 ML Li surface and smallest for the clean surface. This is partly caused by the use of fewer fitting components for the Li-induced surfaces. Other studies show similar results. Kim *et al.*[4] found a bulk component of the same relative intensity on both the 2×2 and the clean surface, but a smaller relative bulk intensity on the 2×1 surface. They explained the difference between the 2×2 and 2×1 surfaces in terms of Li penetration into the surface layers. Also Grehk *et al.*[10] found a larger relative intensity of the bulk component on the clean surface compared to the 2×1:Li surface.

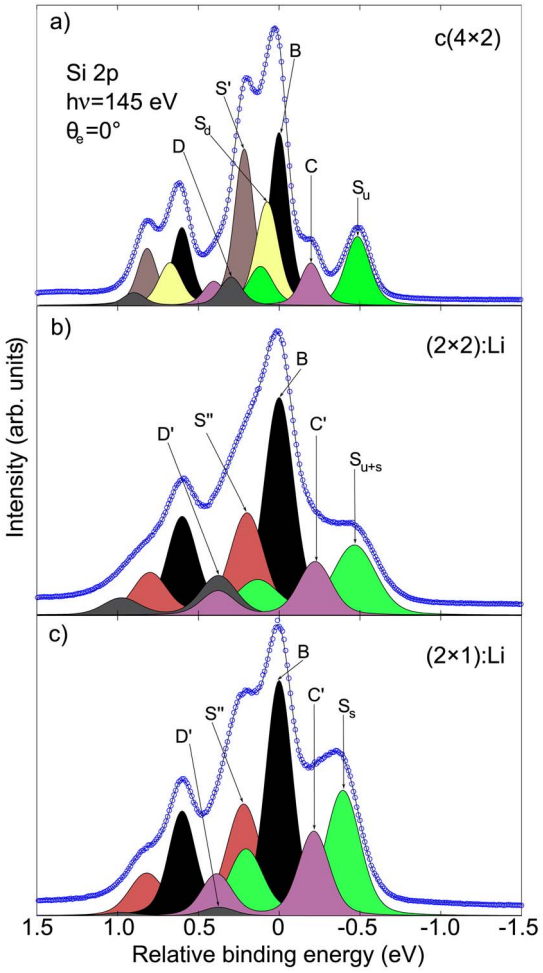

FIG. 10. (Color online) Decomposition of Si 2*p* core level spectra taken at normal emission with a photon energy of 145 eV. (a) Clean $c(4\times2)$, (b) (2×2):Li, (c) (2×1):Li. The binding energies of the different components are relative to the bulk component *B*. Open circles indicate raw data and the solid line is the result of the fit.

The 2×2 structure in Fig. 1(a) exhibits Si dimers with tilt angles of 14.5° and −2.5°. This should be compared to the

19.67° we obtain in calculations for a clean Si(001) $c(4\times2)$ surface. In the core level data of the 2×2 surface the S_{u+s} component is partly attributed to the up atoms of the strongly buckled dimers. The atoms of the weakly buckled dimers are expected to give contributions in the energy range around −0.3 to −0.4 eV and can therefore also contribute to S_{u+s}. In the 2×1 model, Fig. 1(b), the dimers are symmetric and one would therefore only expect a single core level component from the dimer atoms. Comparing the S_u component in Fig. 10(a) with S_{u+s} in Fig. 10(b) and S_s in Fig. 10(c) one notices a shift toward higher binding energy and also an increase in the relative intensity with higher Li coverage. The S_u, S_{u+s}, and S_s components account for 15, 18.5, and 25.5% (0.59, 0.72, and 1 if normalized) of the total intensity for the $c(4\times2)$, 2×2, and 2×1 spectra, respectively. The ratio between the relative intensities is close to what is expected since 50, 75, and 100% (0.5, 0.75, and 1) of the dimer atoms should give contributions in the energy range −0.3 to −0.5 eV for the $c(4\times2)$, 2×2, and 2×1 models, respectively. Both the shifts toward higher binding energy and the increase in relative intensities are therefore consistent with what is expected from the models. The results from the 2×1 surface are in agreement with an earlier core level study by Grehk *et al.*[10] but in disagreement with the core level results by Kim *et al.*[4] where no increase in relative intensity was observed and buckled dimers were suggested for both the 2×2 and 2×1 models.

V. SUMMARY

The 2×2 and 2×1 Si(001):Li surfaces have been investigated with ARPES, high resolution Si $2p$ core level spectroscopy and density functional theory calculations.

ARPES data in the $[\bar{1}10]$ and [110] azimuths are compared to calculated surface state bands by Shi *et al.*[5,9] and to our calculations in the [010] azimuth. Some of the calculated bands in the $[\bar{1}10]$ and [110] azimuths show agreement with experimental data from the 4° off-axis sample with about 80% of the area oriented in same direction. It is, however, often difficult to see the 2×2 or 2×1 symmetry in the experimental dispersions on these surfaces and this makes comparisons difficult. This may be caused by contributions from bulk bands and disturbance from the minority domain.

In the [010] azimuth the edge of the bulk bands disperses strongly downward and leaves the surface state bands in the projected bulk band gap in a large portion of the first SBZ. The experimentally identified 2×2 surface state bands are reproduced in the calculations using the *B*-*T*4 and *P*′-*T*4 models by bands originating mainly from the up atoms of the strongly buckled dimers and down atoms of the weakly buckled dimers. Comparisons are also made using the *B*-*B* and *P*′-*P*′ models which exhibit very similar Si dimer structures but they differ regarding the Li adsorption sites. These models produce surface state bands that are significantly different from those of the *B*-*T*4 and *P*′-*T*4 models and do not reproduce the experimental data.

On the 2×1 surface we observe a single rather sharp feature near $\bar{K}/2$ in the [010] azimuth. This is not consistent with our calculations using the *P*-*T*3′ model which suggest that there should be two or at least one broad feature. Two additional models *P*-*T*3 and *P*-*T*4, are investigated for comparison. The difference between the models is mainly the position of the Li adatom in the trough between the Si dimer rows. The calculated total energy difference is very small between the *P*-*T*3 and *P*-*T*3′ models, the *P*-*T*4 model is significantly higher in energy. Symmetric Si dimers are present in all three 2×1 models with the largest structural difference being the Si dimer bond lengths. The *P*-*T*4 model shows the smallest bond length 2.57 Å, *P*-*T*3′ gives 2.69 Å, and *P*-*T*3 results in the largest bond length 2.78 Å. The experimental data in the [010] azimuth is best replicated by the *P*-*T*3 model. In this model the surface state bands merge at the $\bar{K}/2$ point on the SBZ boundary, see Fig. 9, which explains the observed sharpening of the peak near $\bar{K}/2$ in the ARPES spectra in Fig. 7(b). The surface state bands of the other models remain well separated at the $\bar{K}/2$ point.

In summary, our calculations of the surface band structures along the [010] azimuth for various models of the 2×2:Li and 2×1:Li surfaces have revealed some significant differences. Taking advantage of these differences we have been able to discriminate between the different models by comparing the calculated surface bands to experimental surface state dispersions. We find the best agreement for the *B*-*T*4 and *P*′-*T*4 models of the 2×2:Li surface and for the *P*-*T*3 model of the 2×1:Li surface. The Si $2p$ surface core-level shifts are found to be consistent with the idea of symmetrization of the dimers upon Li adsorption.

ACKNOWLEDGMENTS

Experimental support from T. Balasubramanian and the MAX-lab staff is gratefully acknowledged. This work was financially supported by the Swedish Research Council.

[1] J. D. Levine, Surf. Sci. **34**, 90 (1973).
[2] Y. Enta, T. Kinoshita, S. Suzuki, and S. Kono, Phys. Rev. B **36**, 9801 (1987).
[3] T. Abukawa and S. Kono, Phys. Rev. B **37**, 9097 (1988).
[4] C. Y. Kim, H. W. Kim, J. W. Chung, K. S. An, C. Y. Park, A. Kimura, and A. Kakizaki, Appl. Phys. A **64**, 597 (1997).
[5] H. Q. Shi, M. W. Radny, and P. V. Smith, Phys. Rev. B **69**, 235328 (2004).
[6] Young-Jo Ko, K. J. Chang, and Jae-Yel Yi, Phys. Rev. B **56**, 9575 (1997).
[7] Y. Morikawa, K. Kobayashi, and K. Terakura, Surf. Sci. **283**, 377 (1993).
[8] K. Kobayashi, S. Bügel, H. Ishida, and K. Terakura, Surf. Sci. **242**, 349 (1991).

[9] H. Q. Shi, M. W. Radny, and P. V. Smith, Surf. Sci. **574**, 233 (2005).
[10] T. M. Grehk, L. S. O. Johansson, S. M. Gray, M. Johansson, and A. S. Flodström, Phys. Rev. B **52**, 16593 (1995).
[11] C. Y. Kim, K. S. Shin, K. D. Lee, and J. W. Chung, Surf. Sci. **324**, 8 (1995).
[12] J. P. Perdew, K. Burke, and M. Ernzerhof, Phys. Rev. Lett. **77**, 3865 (1996).
[13] P. Blaha, K. Schwarz, G. K. H. Madsen, D. Kvasnicka, and J. Luitz, WIEN2k, *An Augmented Plane Wave+Local Orbitals Program for Calculating Crystal Properties* (Karlheinz Schwarz, Technische Universität, Wien, Austria, 2001).
[14] H. Koh, J. W. Kim, W. H. Choi, and H. W. Yeom, Phys. Rev. B **67**, 073306 (2003).
[15] E. Landemark, C. J. Karlsson, Y.-C. Chao, and R. I. G. Uhrberg, Phys. Rev. Lett. **69**, 1588 (1992).
[16] O. V. Yazyev and A. Pasquarello, Phys. Rev. Lett. **96**, 157601 (2006).